24th COBEM - 2017

24th ABCM International Congress of Mechanical Engineering
December 3-8, 2017, Curitiba, PR, Brazil

COBEM-2017-2262
MODELLING AND SIMULATION OF A CPV-T SYSTEM

Marianela Machuca Macias
Thiago Henrique Sanaiotto Schmidt
Vinicius de Sousa Britto
Taygoara Felamingo de Oliveira
Antonio C. Pinho Brasil Jr.
University of Brasilia. Mechanical Engineering Department. Energy and Environmental Laboratoty. 70910-900 Brasilia. DF. BRAZIL
nelamacmac@gmail.com, thiagohsschmidt@hotmail.com, viniciusbrto@hotmail.com, taygoara@unb.br, brasiljr@unb.br

Abstract. *The aim of this work is model and simulates a CPV/T system to assess the thermal and electrical efficiencies. A concentrating solar power system concentrates the solar irradiation radiation on photovoltaic cells. The photovoltaic cells are placed under a rectangular duct which contains a cooling fluid used to avoid high temperatures in the photovoltaic cells and to recover some of the energy in the form of thermal energy. A simple heat transfer dimensionless model is implemented in the software MatLab to study the CPV/T system for different operating conditions and different cooling fluids, air, and water. The simulation process allows to define the best configuration of the system and to evaluate its efficiency.*

Keywords: *Solar energy, Concentrating Photovoltaic, CPV-T, Heat recovery*

1. INTRODUCTION

Nowadays, due to greenhouse gases, rising energy demand and market changes in fuel prices. The use and investment in renewable energy are essential to combating climate change and to achieve a more sustainable energy matrix. Solar photovoltaic and concentrated thermal energies, or heliothermic energy, are examples of renewable technologies, as they produce electricity from solar irradiation, a source of clean and inexhaustible energy (Tiwari *et al.*, 2009; Aldegheri *et al.*, 2012).

Photovoltaic systems are becoming cheaper and more diversified and competitive due to the investments made in recent decades. Concentrating photovoltaic systems (CPV) represent an evolution of traditional photovoltaic systems because from an optical system solar radiation is concentrated on the photovoltaic cells, increasing the efficiency of the system (Kurtz, 2009).

On the other hand, the thermal concentrator photovoltaic system (CPV-T) allows the simultaneous generation of electrical and thermal energy, further increasing the overall efficiency of the system because of the cogeneration, the result of the heat transfer used to cool the cells photovoltaic systems and/or to obtain thermal energy. In particular, experimental and theoretical studies were performed to maximize the electrical and thermal efficiencies in this type of systems (Mittelman *et al.*, 2007; Zahedi, 2011; Cheng Qing, 2012; Abu Bakar *et al.*, 2013). Six numerical models were developed by Damir and Mladen. (2012) to describe the effects of design, operation parameters, and mass flow in the technical efficiency of solar collectors. A modeling and design of a CPV-T system for domestic applications was developed by Renno and Petito (2013, 2015) analyzing the choice of a CPV-T system of focal point, and a dynamical simulation using finite elements was performed by Renno and Giacomo (2014).

Specifically, in this work, a simplified dimensionless model of a CPV-T system is addressed. The model is simulated in Matlab with the objective of evaluating the thermal and electrical performances of the photovoltaic concentrator system. The analyzed system is composed of a rectangular duct through which it flows a cooling fluid, air or water, and by photovoltaic cells that will receive the concentrated solar energy of the mirrors, thus producing electric energy. The duct is covered by a thermal insulation to prevent heat loss from the exterior.

The simplified approach is based on a mathematical modeling using dimensionless equations. The CPV-T system is studied for different operating conditions and different cooling fluids in order to know the best configuration and efficiency. Section 2 presents a detailed description of the CPV-T system and the values chosen for the main design parameters. The mathematical model of the system is developed in section 3. In sections 4 and 5 the results and conclusions of the work are presented.

2. CPV-T SYSTEM DESCRIPTION

The CPV-T system simulated in this work uses concentrated solar energy to produce electric energy, through photovoltaic cells, and thermal energy by the transfer of heat to the refrigerant fluid. The system can be divided fundamentally into two subsystems: the concentrator and the receiver. In Fig. 1, the configuration of the CPV-T system to be modeled is presented schematically.

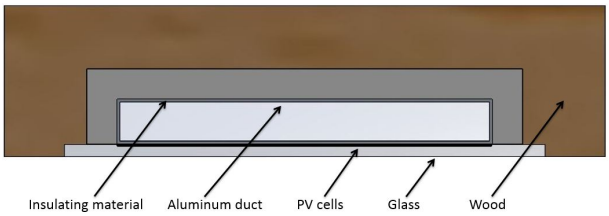

Figure 1. Transversal section of the CPV-T system

The Fresnel linear concentrator is adopted in this work, operating in a similar way to the parabolic mirrors due to the movement of the linear mirrors in relation to the position of the sun. In this case, the solar radiation is reflected from the mirrors to the cells in the absorber, increasing the use of solar radiation. The movement of the mirrors for tracking the sun is an important point to be considered for the purpose of increasing the efficiency of the system. All the mirrors have distinct angulation and a small error in their angulation can result in less solar radiation available to be converted into electrical energy. Only the direct solar radiation can be reflected by the mirrors and in this work it is considered an irradiation of $800W/m^2$, with optical yield of the mirrors, η_{ot} = 0.94 and with factor concentrator F_c = 15.

The receiver is composed of the photovoltaic cells and the cooling system. In this work the performance of the system using water and air as coolant fluids in the heatsink will be analyzed. In order to achieve good efficiency in the photovoltaic system, it is fundamental to dissipate the thermal energy of the cells, since the increase of the temperature in them causes a loss of electrical efficiency.

The photovoltaic cells used are mono-crystalline because of their better efficiencies. According to the manufacturer, the cell has an average efficiency η_{ref} = 22%, for the environment temperature of $Tref$ = $25°C$ and radiation of $1000W/m^2$. The electric efficiency of the cell decays with a rate of β_{ref} = $0.32\%/°C$.

The efficiency of the photovoltaic cells, η_{PV} is calculated according to the equation (Evans and Florschuetz, 1977):

$$\eta_{PV} = \eta_{ref}(1 - \beta_{ref}(T_{PV} - T_{ref})) \tag{1}$$

where T_{PV} is the surface temperature of the cell.

In the absorber, the photovoltaic cells are placed under the duct. Therefore, the area of the absorber is equal to the area occupied by the photovoltaic cells. The chosen cells have dimensions of approximately 125mmx125mm and thickness 0.165mm. In total, 15 photovoltaic cells are placed in series under the duct and the emissivity of ϵ = 0.85 will be considered (Acciani *et al.*, 2010), because the cell exchanges heat through the radiation with the external medium.

The duct used is of aluminum and is covered with an insulating material of 50 mm thickness. The thermal conductivity of the aluminum is k_a = $204W/mK$, and the insulation, k_i = $0.03W/mK$. The value of the mass flow inside the tube was considered to be between 0.01 and $0.05kg/s$ as used in the literature. The glass is used under the cells to protect them from the external environment and because of that part of the energy that reaches the receiver is reflected in the glass back to the atmosphere before reaching the cells. The commercial glass used has the transmissivity equal to τ_g = 0.82, the absorptivity equal to α_g = 0.11, the reflectivity equal to ρ = 0.7 and the thermal conductivity of k_g = $1.4W/mK$.

In Tab. are collected all the parameters and characteristics of the material used.

Table 1. Thickness and thermal conductivity values referent to the material used in the system (Boltz, 1973; Fellini, 2007)

	Thickness [mm]	Thermal conductivity k $[W/m.K]$
Glass	5.0	1.4
Photovoltaic cell	0.165	148.0
Aluminum	0.5	204.0
Insulating	10.0	0.028
Wood	10.0	0.3

Table 2. Emissivity, absorptivity and transmissivity values referent to the material used in the system (de P. Nicolau and Maluf, 2001)

	Emissivity	Absorptivity	Transmissivity
Glass	0.90	0.11	0.82
Photovoltaic cell	0.85	0.92	0.00
Aluminum	0.04	-	-
Wood	0.90	0.30	0.00

As previously mentioned, this paper deals with the simplified modeling of a CPV-T system. In the case of studying a more realistic system, it is necessary to consider the existence of a material between the cells and the aluminum duct, as for example a thermal paste, to avoid the short circuit.

3. MATHEMATICAL MODEL

In this section is presented the mathematical model for a CPV-T system described in the section 2. A energy balance is realized in the different parts of the system: receiver (glass), fluid and insulator element. The mathematical model consists of a dimensionless system equations where the unknowns of the system are the temperatures of the elements, photovoltaic cells and fluid. The dimensionless equations allows to analyze the variable and parameters of the problem more easily.

The Fig.(2) shows the heat exchange on each element of the system. A fraction of the energy received by the system is converted into electrical energy by the photovoltaic cells and in thermal energy increasing the temperature of the fluid flowing by the duct. Inside the duct, the radiation and convection heat exchange were contemplated.

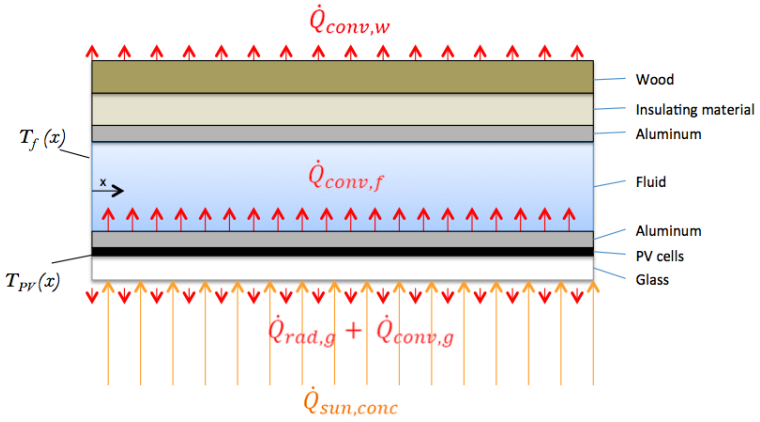

Figure 2. Model system to heat transfer

The energy balance on the system is expressed in the Eq.(2) as

$$\dot{Q}_{thermal} = \dot{Q}_{cond,g} + \dot{Q}_{cond,d} + \dot{Q}_{conv,f} + \dot{Q}_{rad,g} + \dot{Q}_{conv,g} \tag{2}$$

where $\dot{Q}_{conv,f}$ and $\dot{Q}_{conv,g}$ represent the convection heat exchange between duct and fluid, and glass and environmental, respectively. The $\dot{Q}_{conv,w}$ is the heat transfer by convection between the surface of wood and the environment. The $\dot{Q}_{rad,g}$ is the radiation heat exchange between the glass and the environmental. The conduction heat in the glass and the duct are represented as $\dot{Q}_{cond,g}$ and $\dot{Q}_{cond,d}$.

Finally, $\dot{Q}_{thermal}$ is the energy dissipated by the photovoltaic cells and is expressed as the sum the dissipated energies on the cells and the glass, $\dot{Q}_{\alpha}$. The cell efficiency, η_{PV}, varies with the temperature, therefore, along the concentrator system. The Eq. (1) shows that dependency between efficiency and temperature.

$$\dot{Q}_{thermal}(x) = \dot{Q}_{\tau}(1 - \eta_{PV}(x)) + \dot{Q}_{\alpha} \tag{3}$$

The energy which incident on the system, $\dot{Q}_{system}$, is converted in electric and thermal energy, $\dot{Q}_{\tau}$. $\dot{Q}_{\tau}$ is the solar radiation that is flows through the glass and $\dot{Q}_{\alpha}$ is the fraction of the energy dissipated in the glass. So that, $\dot{Q}_{\alpha} = \dot{Q}_{system} - \dot{Q}_{\tau}$.

The $\dot{Q}_{system}$ and $\dot{Q}_{\tau}$ are defined as showed in the Eq. (4) and Eq. (5)

$$\dot{Q}_{system} = \dot{Q}_{sun,conc}\psi_m N_m A_m \alpha_{PV}(\tau_g + \alpha_g) \tag{4}$$

$$\dot{Q}_{\tau} = \dot{Q}_{sun,conc}\psi_m N_m A_m \tau_g \tag{5}$$

where N_m and A_m are the number and the area of the mirrors and ψ_m is the reflectivity of the mirrors. On the other hand, τ_g and α_g are the transmissivity and absorptivity of the glass. The absorptivity of the photovoltaic cells is α_{PV} and the $\dot{Q}_{sun,conc}$, the direct solar radiation concentrated by the mirrors incident on the glass.

The other energy balance is carried out on the fluid, Eq. (6).

$$\dot{Q}_{fluid}(x) = \dot{m}Cp\Delta T \tag{6}$$

where $\dot{m}$ is the mass flow $[kg/s]$ and Cp the specific heat $[J/kg°C]$.

The flow inside the duct absorb a heat fraction through convection between the flow and duct, $\dot{Q}_{conv,f}$, cooling the system and helping to photovoltaic cells keeping the temperature not too high for so as not to impair efficiency. A fraction of that energy is transmitted to the duct,$\dot{Q}_{cond,d}$, and the insulator walls by conduction, $\dot{Q}_{cond,i}$, being therefore, dissipated to the environmental by conduction and convection in the wood wall, $\dot{Q}_{cond,w}$ and $\dot{Q}_{conv,w}$.

$$\dot{Q}_{fluid}(x) = \dot{Q}_{conv,f} + \dot{Q}_{cond,d} + \dot{Q}_{cond,i} + \dot{Q}_{cond,w} + \dot{Q}_{conv,w} \tag{7}$$

Next, the equations for conduction, convection and radiation are substituted in the balance equations, Eq. (2) and Eq. (7), and the dimensionless is realized.

$$\dot{Q}_{cond} = -\frac{kA\Delta T}{e} \tag{8}$$

$$\dot{Q}_{rad} = \epsilon\sigma A T^4 \tag{9}$$

$$\dot{Q}_{conv} = hA\Delta T \tag{10}$$

In order to obtain the system of equations which model the problem are defined dimensionless variables. The dimensionless temperature, $\tilde{T}$ is determinate as

$$\tilde{T} = \frac{T}{T_\infty} \tag{11}$$

The ratio between the solar radiation, G, and σT_∞^4 was considered being Π_{sun} and the relation between the heat transfer coefficient as Π_{conv}

$$\Pi_{sun} = \frac{G}{\sigma T_\infty^4} \tag{12}$$

$$\Pi_{conv} = \frac{h_{conv,w}}{h_{conv,f}} \tag{13}$$

The heat transfer dimensionless numbers used are the Biot number, Bi, the Nusselt number and the Hottel number, Hot. The Hottel number was defined as the ratio between the convective and radiative flow by Hottel and Sarofim (1967).

$$Bi = \frac{h\delta}{k} \tag{14}$$

$$Hot = \frac{h}{\sigma T_{\infty}^3} \tag{15}$$

The Nusselt number is calculated using empirical correlations found in the literature and it is expressed as

$$Nu = \frac{hL}{k} \tag{16}$$

In order to compute the heat transfer coefficient, h, the Nusselt numbers are calculated using empirical correlations found in the literature (McAdams, 1954; Incropera and Dewitt D., 2011). In external convection the heat transfer coefficient is determinate using the empirical correlation to horizontal flat plate

$$Nu_{\delta} = 0.27 Ra_L^{1/4} \tag{17}$$

when the Rayleight number, Ra, is $10^5 \leq Ra_L \leq 10^10$. Being defined the Rayleigh number as

$$Ra \equiv \frac{g\beta_T (T - T_{\infty}) L^3}{\nu^2} \tag{18}$$

and for the vertical external surfaces is used the next correlation

$$Nu_{_{\delta}} = \left[0,825 + \frac{0,387 Ra_{_L}^{1/6}}{\left[1 + \left(\frac{0,492}{Pr_{ar}}\right)^{9/16}\right]^{8/27}} \right]^2 \tag{19}$$

The external forced convection is used the correlation for horizontal flat plate with transition flow from laminar to turbulent, as

$$Nu_{for} = 0.68 Re^{1/2} Pr^{1/3} \tag{20}$$

In real situations, free and forced convections effects are observed. Therefore, the Nusselt number in external convection is expressed as a combination between Nu in free convection,Nu_{δ}, and Nu in forced convection, Nu_{for}, as shown in the Eq. 21

$$Nu_{conv}^{e} = \left(Nu_{\delta}^{3.5} + Nu_{for}^{3.5}\right)^{1/3.5} \tag{21}$$

In order to determinate the internal heat transfer coefficient are computed the Nu numbers to free and forced convection inside the duct. A simplified way to calculate the Nu number in natural convection when the flow is laminar and the Ra number is between $10^6 < Ra < 10^9$ and $1 < L/\delta < 40$ (Incropera and Dewitt D., 2011) is expressed in Eq. 22, being L and δ the length and high of the duct, respectively.

$$Nu_{\delta} = 0,046 Ra^{1/3} \tag{22}$$

In forced convection in ducts where the flow is laminar and one surface presents a heat flow and the other are insulated the Nu number can be simplified as a constant like

$$Nu_{for} = 5.385. \tag{23}$$

Thus, the Nusselt number is also calculated in a combined manner, as previously shown in the case of external convection.

$$Nu_{conv}^{i} = \left(Nu_{\delta}^{3.5} + Nu_{for}^{3.5}\right)^{1/3.5} \tag{24}$$

Finally, after the substitutions of conduction, radiation and convection equations in the energy balance equations and realized the dimensional analyze are obtained the equation which model the system. Therefore,

$$\epsilon_{PV}\tilde{T}_{PV}^4 + \left[Hot_{conv,g}\left(2+\frac{1}{Bi_g}\right)+\frac{Hot_{conv,f}}{Bi_d}\right]\tilde{T}_{PV} - Hot_{conv,g}\tilde{T}_f - \epsilon_{PV} - Hot_{conv,g}\left(\frac{1+Bi_g}{Bi_g}\right) - \frac{Hot_{conv,f}}{Bi_d} - \Pi_{sun}n_m\phi_m A_m\left[\tau_g\left(1-\eta_{PV}(x)\right)-\alpha_g\right] = 0, \tag{25}$$

Similarly, the Eq. (26) is obtained,

$$\frac{d\tilde{T}_f}{d\tilde{x}} = \left(2+Bi_i+Bi_w+Bi_d+\Pi_{conv}\right)\tilde{T}_{PV} - \tilde{T}_f - \left(1+Bi_i+Bi_w+Bi_d+\Pi_{conv}\right) \tag{26}$$

defining the characteristic length as $x = \tilde{x}\dfrac{\dot{m}C_p}{h_{conv,f}w} = \tilde{x}L_c$, being w the wide of the duct.

In order to compute the electrical, $\eta_e(x)$, thermal, $\eta_t(x)$, and systen efficiencies, $\eta_{system}(x)$, are used the following equations,

$$\eta_e(x) = \frac{\eta_{pv}\dot{Q}_\tau}{\dot{Q}_{system}} \tag{27}$$

$$\eta_t(x) = \frac{\dot{Q}_{fluid}(x)}{\dot{Q}_{system}(x)} \tag{28}$$

$$\eta_{system}(x) = \eta_e(x) + \eta_t(x) \tag{29}$$

4. RESULTS

This section presents the results obtained from using air and water as a coolant fluid in a CPV/T system.

The Newton-Raphson numerical method was used to resolve the equation system calculating the temperature of the cells, T_{PV}, and also of the fluid, T_f, through the iterative process. Using these temperatures, the thermal and electrical efficiency was computed for different fluids and mass flows. The study was conducted in the city of Brasilia, where the local temperature $T_\infty = 293K$, relative humidity is equal to 50%, local wind speed is $u_\infty = 1m/s$ and direct radiation is equal to $800W/m^2$.

The dimensions of the solar system are presented in the Tab. 3

Table 3. Dimensions of the materials used in the CPV-T system

Dimensions [mm]	Length	Width	Thickness
Glass	1500	125	5,0
Photovoltaic Cell	125	125	0,165
Duct	1500	125	1,0
Insulator	1500	125	10,0
Wood	1500	125	10,0

The CPV-T system has 15 mirrors (totaling $0.1875m^2$) which receive 2250.0W of radiation, but around 6% is dissipated in the mirrors. In the glass, around 7% of the energy is reflected back to the external environment, mainly because of the angle of incidence of the solar rays in relation to the flat surface of the glass. Thus, the incoming energy is 1967.0J every second, about 87.42% of the concentrated radiation. The Tab. 4 exhibits the solar energy distribution on the system in the starting operation, considering the photovoltaic cell efficiency of 22%. That value will decrease with the increase of the temperature of the photovoltaic cells.

Table 4. Solar energy distribution in the starting operation

	$\dot{Q}_{sun}$	$\dot{Q}_{system}$	$\dot{Q}_{thermal}$	$\dot{Q}_{eletrical}$
Energy [J]	2250,0	1967,0	1585,4	379,4
Percentage [%]	100	87,42	70,46	16,96

In order to analyze the consequences that the increase of mass flow causes in the extraction of thermal energy from the photovoltaic cells, the mass flows (air and water) equal to 0.01 and 0.025 kg / s were used during the simulations.

4.1 Air cooling

The Fig. 4.1 displays the temperature of the fluid and the photovoltaic cells using air as a cooling flow for the mass flow equal to 0.01 and 0.025 kg/s.

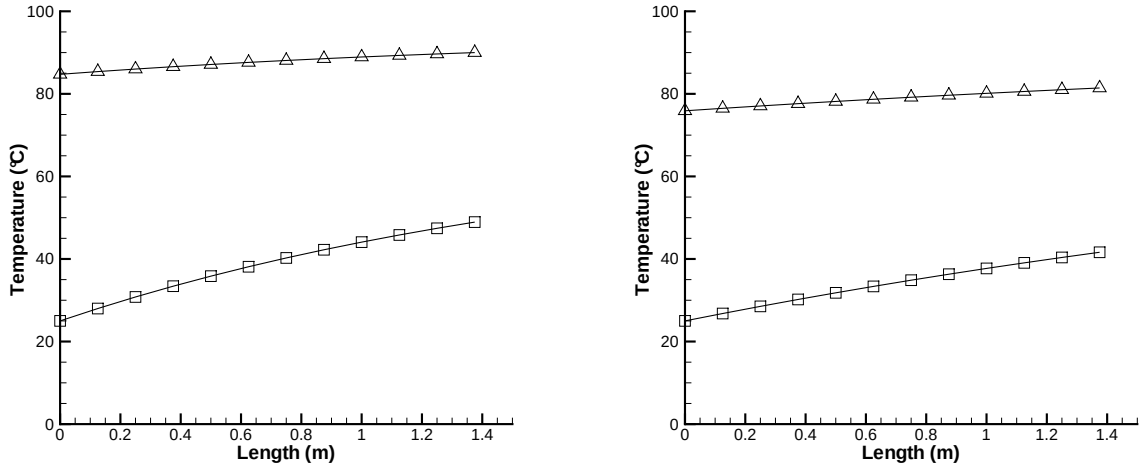

(a) $\dot{m}$ = $0.01kg/s$ (b) $\dot{m}$ = $0.025kg/s$

Figure 3. Temperatures when used air cooling - Δ Photovoltaic cell temperature and □ Fluid temperature

It can be observed the difference of temperatures, between the photovoltaic cells and the fluid, decrease when the mass flow increases. Thus, the increasing of the flow velocity inside of the duct intensifies the heat transfer between the fluids and the PV cells due to the increase of the convective constant. Consequently, the PV cell temperature decreases but held high, around $80°C$, so the cell's electrical efficiency is well below 22% (electrical efficiency for $25°C$), as can be seen in the Fig. 4.1. Also, it can be observed the values of the thermal, electrical and system efficiency with air-cooling. It's noted that the electric efficiency is close to 16%, in both of cases, but when the air mass flow increases its thermal efficiency goes from 18 to 28% . It occurs due to the removed heat from the cells when the mass flow increases from 0.01 to 0.025kg/s.

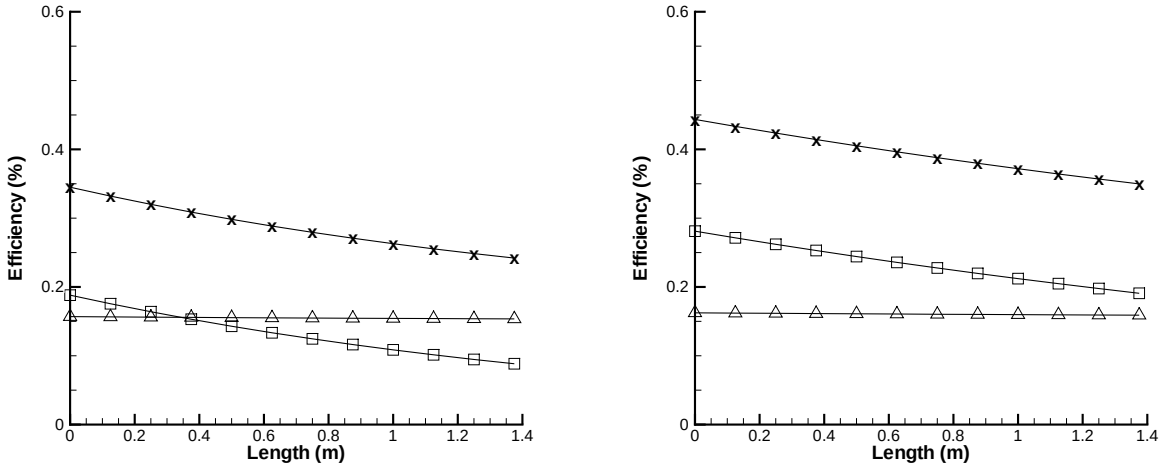

(a) $\dot{m}$ = $0.01kg/s$ (b) $\dot{m}$ = $0.025kg/s$

Figure 4. System efficiencies using air cooling - Δ Electrical efficiency, □ Thermal efficiency and x System efficiency.

The decrease of the thermal efficiency as shown in Fig. 4(a) and Fig. 4(b) is caused by the saturation of the air in

absorbing heat from the PV cells, which results in dissipation of heat from the fluid to the walls of the insulation due to high working temperature.

The Tab. 5 and the Tab. 6 show the outlet temperatures in the system and the flow velocities depending of the mass flow used and the system efficiencies, respectively.

Table 5. Outlet temperatures in the CPV-T using air cooling

Mass flow $[kg/s]$	u $[m/s]$	T_{PV} $[°C]$	T_f $[°C]$
$\dot{m}$ = 0.01	6.1	90.0	48.9
$\dot{m}$ = 0.025	15.2	81.4	41.6

Table 6. System efficiencies using air cooling

Mass flow $[kg/s]$	u $[m/s]$	$\eta_{thermal}[\%]$	$\eta_{eletrical}[\%]$	$\eta_{system}[\%]$
$\dot{m}$ = 0.01	6.1	18.81	15.69	34.50
$\dot{m}$ = 0.025	15.2	28.11	16.24	44.35

As commentated previously, the thermal efficiency goes from 18.81% to 28.11% after incrementing the mass flow inside the duct while the variation in the electrical efficiency is not significant. The system efficiency also increases in case of higher mass flow. However, it is not viable to increase the mass flow to higher values because it will be required a pump with high power, resulting in a higher price to pump the air.

4.2 Water cooling

As in the previous study for air-cooling, it was also used the mass flows of 0.01 and 0.025 kg/s for water-cooling.

Due to the water has a thermal conductivity greater than the air and a high convection coefficient, the difference of temperature between the fluid and cells (Fig. 4.2) is smaller than the same difference in the case of the air mass flow (Fig. 4.1). Therefore, it is evident that the selection of the coolant fluid is an important parameter. The lower the difference of temperature between the cells and the fluid, the more thermal energy the fluid absorbs from the photovoltaic cells and consequently the electrical efficiency increases.

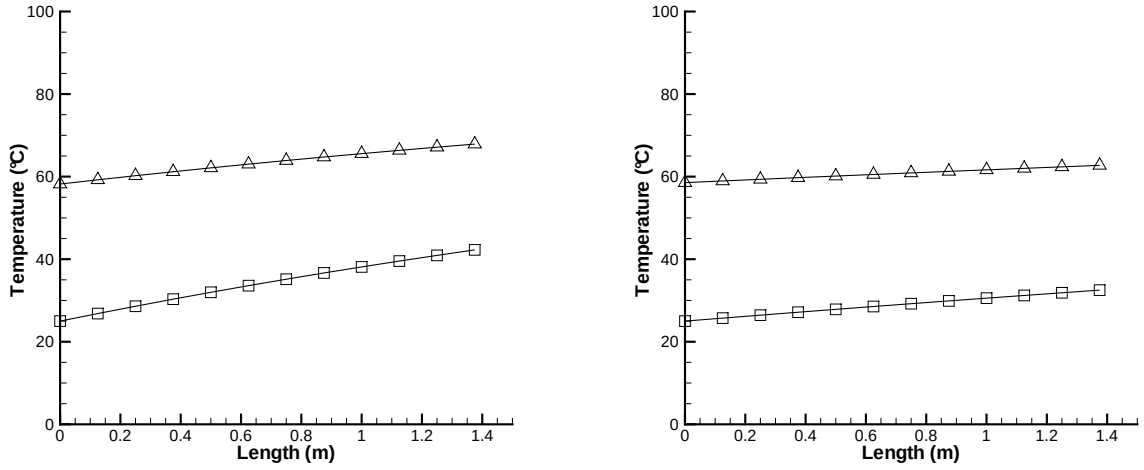

(a) $\dot{m}$ = $0.01kg/s$ (b) $\dot{m}$ = $0.025kg/s$

Figure 5. Temperatures when used water cooling - Δ Electrical efficiency, □ Thermal efficiency and x System efficiency.

It is noticed that the temperature of the cells decreases to between 60-70$°C$ with the use of water as a coolant. As a consequence, he electric efficiency is close to 17%, in both of cases, and the thermal efficiency to more than 45%. The combined efficiency of 63.55% is obtained for a mass flow of 0.01kg/s and 63.93% for 0.025kg/s, as exhibited in Fig. (4. 2).

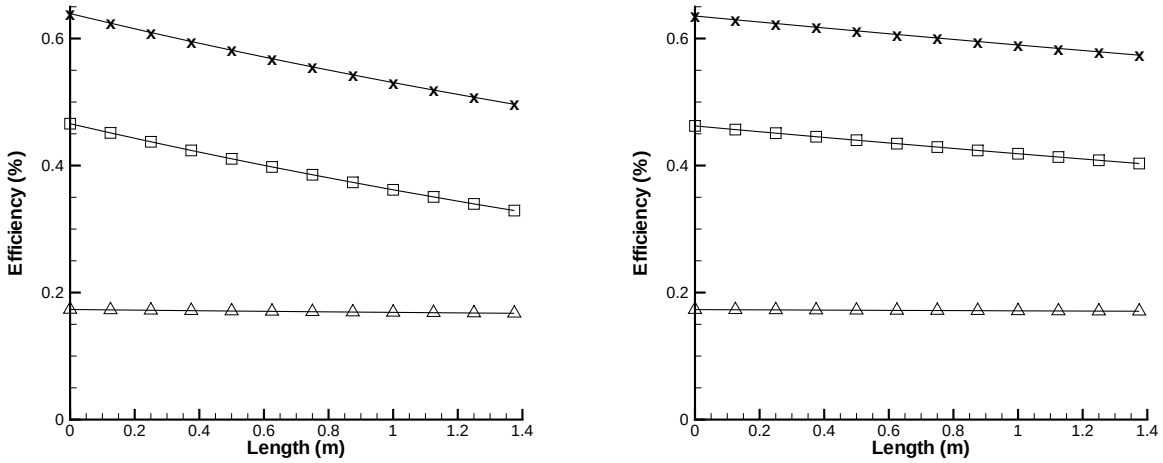

(a) $\dot{m}$ = $0.01kg/s$ (b) $\dot{m}$ = $0.025kg/s$

Figure 6. System efficiencies using water cooling - Δ Electrical efficiency, □ Thermal efficiency and x System efficiency.

The Tab. 7 and the Tab. 8 show the outlet temperatures in the system (higher temperature), the velocities of flow, and the higher efficiencies. The values of the efficiencies were obtained in the beginning of the duct because the more the fluid flows inside of the duct, the more thermal energy is absorbed. Consequently the thermal and electrical efficiencies are higher in the beginning of the duct and the temperatures are higher at the end of the duct.

Table 7. Outlet temperatures in the CPV-T using water cooling

Mass flow $[kg/s]$	u $[m/s]$	T_{PV} $[°C]$	T_f $[°C]$
$\dot{m}$ = 0.01	0.0063	69.9	42.3
$\dot{m}$ = 0.025	0.016	62.7	32.5

Table 8. System efficiencies using water cooling

Mass flow $[kg/s]$	u $[m/s]$	$\eta_{thermal}[\%]$	$\eta_{eletrical}[\%]$	$\eta_{system}[\%]$
$\dot{m}$ = 0.01	0.0063	46.24	17.34	63.93
$\dot{m}$ = 0.025	0.016	46.93	17.32	63.55

5. CONCLUSIONS

The main conclusion of this study is that when tested in the same conditions, water proves to be more efficient than air in absorbing heat. When mass flow is equal to 0.01kg/s, water reaches a total efficiency of 63%, compared efficiency reaching 34% via air-cooling. The increase of mass flow for both fluids increased thermal efficiency because the heat transfer due to convection between the fluid and the cells is directly proportional to the mass flow. In this study it was also possible to monitor the temperature of the cells for different fluids and mass flows, and consequently analyze the electrical efficiency because it is indirectly proportional to the temperature.

6. ACKNOWLEDGEMENTS

This work is partially financed by the JAIBA Solar R&D project (ANEEL Strategic Grant 013/2011) and supported by CERAN and ELETROBRAS-FURNAS.

7. REFERENCES

Abu Bakar, M.N., Othman, M., Hj Dina, M., Manaf, N.A. and Jarimi, H., 2013. "Design concept and mathematical model of a bi-fluid photovoltaic/thermal (PV/T) solar collector". *Renew Energy 2013:1e12. xxx.*

Acciani, G., Falcone, O. and Vergura, S., 2010. "European association for analysis of the thermal heating of poly-si and a-si photovoltaic cell by means of fem". Vol. 1.

Aldegheri, F., Baricordi, S., Bernardoni, P., Brocato, M., Calabrese, G., Guidi, V., Mondardini, L., Pozzetti, L., Tonezzer, M. and Vincenzi, D., 2012. "Building integrated low concentration solar system for a self-sustainable mediterranean villa: the astonyshine house,". *Energy Build. 77*, pp. 355–363.

Boltz, E.R., 1973. *CRC handbook of tables for applied engineering science. [*. [S.I.].

Cheng Qing, Zhang Xiao-Song, L.X.W., 2012. "Double-stage photovoltaic/thermal ed regeneration for liquid desiccant cooling system." *Energy Build*.

Damir, D. and Mladen., A., 2012. "Numerically assisted analysis of flat and corrugated plate solar collectors thermal performances". *Sol Energy*, Vol. 86, pp. 2416–2431.

de P. Nicolau, V. and Maluf, F.P., 2001. "Determination of radiative properties of commercial glass". *PLEA 2001 - The 18th Conference on Passive and Low Energy Architecture, Florianopolis âĂŞ BRAZIL, 7-9 November 2001*.

Evans, D. and Florschuetz, L., 1977. "Cost studies on terrestrial photovoltaic power systems with sunlight concentration." *Solar Energy*, Vol. 19, No. 3, pp. 255–262.

Fellini, R., 2007. "Sistemas termoisolantes: tipos, finalidades e aplicacao". *Revista Climatizacao e Refrigeracao*.

Hottel, H. and Sarofim, A., 1967. *Radiative transfer*. McGraw-Hill Book Company.

Incropera, F.P. and Dewitt D., P., 2011. *Fundamentals of Heat and Mass Transfer*. John Wiley & Sons, 7th edition.

Kurtz, S., 2009. "Opportunities and challenges for development of a mature concentrating photovoltaic power industry, u.s." Technical report, Department of Energy, Technical Report, NREL/TP-520-43208.

McAdams, W.H., 1954. *Heat transmission.* [S.l.].

Mittelman, G., Kribus, A. and Dayan, A., 2007. "Solar cooling with concentrating photovoltaic/thermal (CPV/T) systems." *Energy Conversion And Management*, Vol. 48, pp. 2481–2490.

Renno, C. and Giacomo, M.D., 2014. "Dynamic simulation of a cpv/t system using the finite element method,". *Energies*, Vol. 7, pp. 7395–7414.

Renno, C. and Petito, F., 2013. "Design and modeling of a concentrating photovoltaic thermal (CPV/T) system for a domestic application". *Energy and Buildings*, Vol. 62, pp. 392–402.

Renno, C. and Petito, F., 2015. "Choice model for a modular configuration of a point-focus CPV/T system". *Energy and Buildings*, Vol. 92, pp. 55–66.

Tiwari, A., Dubey, S., Sandhu, G.S., Sodha, M.S. and Anwar, S.I., 2009. "Exergy analysis of integrated photovoltaic thermal solar water heater under constant flow rate and constant collection temperature modes." *Applied Energy*, Vol. 86, pp. 2592–2597.

Zahedi, A., 2011. "Review of modeling details in relation to low-concentration solar concentrating photovoltaic,". *Renewable Sustainable Energy Review*, Vol. 15, pp. 1609–1614.

8. RESPONSIBILITY NOTICE

The authors are the only responsible for the printed material included in this paper.